

Silent Scaffolds

INHIBITION OF *c-Jun* N-TERMINAL KINASE 3 ACTIVITY IN CELL BY DOMINANT-NEGATIVE ARRESTIN-3 MUTANT[§]

Received for publication, March 2, 2012, and in revised form, April 18, 2012. Published, JBC Papers in Press, April 20, 2012, DOI 10.1074/jbc.M112.358192

Maya Breitman, Seunghyi Kook, Luis E. Gimenez, Britney N. Lizama, Maria C. Palazzo, Eugenia V. Gurevich, and Vsevolod V. Gurevich¹

From the Department of Pharmacology, Vanderbilt University, Nashville, Tennessee 37232

Background: JNK kinases play an important role in cell death and differentiation.

Results: Arrestin-3 mutant that binds ASK1, MKK4, and JNK3 normally without promoting JNK3 activation suppresses JNK3 activation in the cell.

Conclusion: Modified scaffolding proteins can be used to regulate MAP kinase activity *in vivo*.

Significance: Silent scaffolds are a novel type of molecular tool for manipulation of MAP kinase activity in cells.

We established a new *in vivo* arrestin-3-JNK3 interaction assay based on bioluminescence resonance energy transfer (BRET) between JNK3-luciferase and Venus-arrestins. We tested the ability of WT arrestin-3 and its 3A mutant that readily binds β 2-adrenergic receptors as well as two mutants impaired in receptor binding, Δ 7 and KNC, to directly bind JNK3 and to promote JNK3 phosphorylation in cells. Both receptor binding-deficient mutants interact with JNK3 significantly better than WT and 3A arrestin-3. WT arrestin-3 and Δ 7 mutant robustly promoted JNK3 activation, whereas 3A and KNC mutants did not. Thus, receptor binding, JNK3 interaction, and JNK3 activation are three distinct arrestin functions. We found that the KNC mutant, which tightly binds ASK1, MKK4, and JNK3 without facilitating JNK3 phosphorylation, has a dominant-negative effect, competitively decreasing JNK activation by WT arrestin-3. Thus, KNC is a silent scaffold, a novel type of molecular tool for the suppression of MAPK signaling in living cells.

Arrestins bind active phosphorylated forms of their cognate G protein-coupled receptors, shutting down G-protein activation and redirecting signaling to alternative pathways (1, 2). Mammals have four arrestin subtypes, two of which, arrestin-1² and -4, are expressed in photoreceptor cells. Non-visual arrestin-2 and -3 are expressed in virtually every cell in the body and function as versatile regulators of cell signaling, interacting with dozens of non-receptor partners, such as MAP³ kinases (3,

4). Typical MAP kinase cascades consist of three kinases that successively phosphorylate and activate the downstream component. In many cases the activation of MAP kinase cascades is controlled by the binding of all three kinases to a scaffolding protein (5, 6). In response to G protein-coupled receptor activation, arrestins scaffold three main MAP kinase cascades, facilitating the activation of JNK3 (7), ERK1/2 (8), and p38 (9).

The activity of JNK family kinases sends anti-proliferative, often pro-apoptotic signals to the cell. JNK signaling was implicated in many disorders and represents an inviting target for therapeutic intervention (10). Arrestin-3 binds ASK1, MKK4, and JNK3 and promotes JNK3 activation (7, 11–14). Interestingly, all four mammalian arrestins bind these kinases (12, 15–17), but even highly homologous arrestin-2 does not facilitate JNK3 activation (11, 12). Thus, binding *per se* does not necessarily translate into productive scaffolding, suggesting that to facilitate signaling in this cascade, arrestin needs to hold the kinases in an optimal orientation. Recently we identified several arrestin-3 mutants that bind ASK1, MKK4, and JNK3 at least as well as wild type (WT) arrestin-3 but fail to facilitate JNK3 phosphorylation in the cell (13). These findings suggest the possibility of designing a “silent scaffold,” *i.e.* an arrestin that binds the kinases well enough to compete with other scaffolds and holds them in an unproductive complex, thereby decreasing JNK activity in the cell. Here we provide the first demonstration that this mechanism of MAPK regulation works in living cells. We show that an arrestin-3 mutant that tightly binds upstream kinases and JNK3 without facilitating its phosphorylation acts in a dominant-negative fashion, competitively decreasing JNK3 activation by an active scaffold, WT arrestin-3. Silent scaffold is a novel type of molecular tool for the manipulation of MAPK signaling, which can be used for scientific and therapeutic purposes.

EXPERIMENTAL PROCEDURES

Materials—All restriction and DNA modifying enzymes (T4 DNA ligase, Vent[®] DNA polymerase, and calf intestine alkaline phosphatase) were from New England Biolabs (Ipswich, MA). Cell culture reagents and media were from Mediatech (Manassas, VA) or Invitrogen. The luciferase substrate coelentera-

* This work was supported, in whole or in part, by National Institutes of Health Grants GM081756, GM077561, and EY011500 (to V. V. G.) and NS065868 (to E. V. G.).

[§] This article contains supplemental Fig. S1.

¹ To whom correspondence should be addressed. Tel.: 615-322-7070; Fax: 615-343-6532; E-mail: vsevolod.gurevich@vanderbilt.edu.

² We use systematic names of arrestin proteins: arrestin-1 (historic names S-antigen, 48-kDa protein, visual or rod arrestin), arrestin-2 (β -arrestin or β -arrestin1), arrestin-3 (β -arrestin2 or hTHY-ARRX), and arrestin-4 (cone or X-arrestin; for unclear reasons its gene is called “arrestin 3” in the HUGO database).

³ The abbreviations used are: MAP, mitogen-activated protein; β 2AR, β 2 adrenergic receptor; β 2AR-RLuc8, β 2AR tagged with C-terminal *Renilla* luciferase variant 8; BRET, bioluminescence resonance energy transfer; ANOVA, analysis of variance.

JNK Inhibition by Silent Scaffold

zine-h was from DiscoverX (Fremont, CA). All other reagents were from Amresco (Solon, OH) or Sigma.

Cell Culture and Transient Transfection—COS-7 cells were maintained in Dulbecco's modified Eagle's medium supplemented with 10% fetal bovine serum (Invitrogen), penicillin, and streptomycin at 37 °C in a humidified incubator with 5% CO₂. The cells at 80–90% confluence were transfected using Lipofectamine 2000 (Invitrogen) (3 μl per 1 μg of DNA). The next day the cells were seeded onto 96-well plates for bioluminescence resonance energy transfer (BRET) measurements and onto 6-well plates for Western blot analysis.

Plasmids and Mutagenesis—The plasmids encoding arrestins N-terminal-tagged with Venus in a modified pcDNA3 (Invitrogen) (12) were constructed as described (18, 19). RLuc8 was fused in-frame with the triple HA-tagged human β2 adrenergic receptor (β2AR) (cDNA resource center) as described (18). The coding sequence of the prevalent short splice variant of bovine arrestin-3 (20) with or without a C-terminal FLAG tag (15) was subcloned into pcDNA3 (21). Three arrestin-3 mutants were used: (a) 3A, a “constitutively active” form with a triple alanine substitution (I386A, V387A, F388A) that detaches the C-tail from the body of the molecule (22) with enhanced binding to active phosphorylated and unphosphorylated G protein-coupled receptors (23); (b) Δ7, with a seven-residue deletion in the interdomain hinge that “freezes” arrestin-3 in the basal conformation and impairs its ability to bind receptors (12, 24); (c) KNC, with 12 alanine substitutions of the key receptor binding residues (K11A, K12A, L49A, D51A, R52A, L69A in the N-domain and Y239A, D241A, C252A, P253A, D260A, Q262A in the C-domain) that retains normal conformational flexibility but does not bind receptors (18, 25). The coding sequences of human JNK3α2 and its ΔN mutant (lacking residues 2–39) that does not bind arrestins (12) were amplified by PCR with the addition of EcoRI and Sbf I sites and fused in-frame with the C-terminal *Renilla* luciferase variant 8 (26). All constructs were verified by dideoxy-sequencing.

Western Blotting, MAPK Activity, and Stimulation—For JNK3α2 and ERK1/2 phosphorylation assays, 24 h after transfection cells were serum-starved overnight and treated for 8 min at 37 °C with 10 μM β2AR agonist isoproterenol or 1 μM ICI118551, an inverse agonist for G proteins and biased agonist for arrestins (27). Cells were washed with PBS and solubilized in lysis buffer containing protease (Complete mini, Roche Applied Science) and phosphatase (PhosSTOP, Roche Applied Science) inhibitor cocktails as described (28). Protein was measured using the Bio-Rad Coomassie Blue assay. The proteins were resolved on 10% SDS-PAGE and transferred to polyvinylidene difluoride membranes (Millipore, Bedford, MA). Blots were incubated with the primary antibodies (Cell Signaling Technology, Inc) anti-phospho-JNK, anti-p44/42 phospho-ERK1/2, anti-p44/42 ERK1/2, anti-HA (6E2) (1:1000 to 1:5000), and GAPDH (Millipore) (1:500) followed by appropriate HRP-conjugated secondary antibodies. Arrestins were visualized with F4C1 mouse monoclonal antibody (29) (1:10,000). Protein bands were detected by enhanced chemiluminescence (ECL, Pierce) and x-ray film.

BRET Assays; Arrestin-β2AR Interactions—COS-7 cells were transfected in 60-mm dishes with 0–12 μg of Venus-arrestin

constructs along with 125 ng of β2AR-RLuc8 plasmid and empty pcDNA3 to equalize DNA. After 24 h cells were reseeded at 100,000 to 200,000 cells per well onto white opaque 96-well microplates (Nunc, Rochester, NY) for luminescence or black opaque microplates (Nunc) for fluorescence measurements. Forty-eight hours after transfection, the medium was replaced with PBS with Ca²⁺ and Mg²⁺ containing 0.01% glucose (w/v), 36 mg/liter sodium pyruvate, and 25 mM HEPES-Na, pH 7.2. Coelenterazine-h (DiscoverX, Fremont, CA) at 5 μM was added 8 min after agonist (25 μM isoproterenol), and luminescence was measured using Synergy 4 microplate reader (BioTek, Winooski, VT). The light emitted by coelenterazine-h and Venus in each well was measured for 1 s through 460- and 535-nm filters. The BRET ratio was calculated as the long wavelength emission divided by the short wavelength emission. The expression of Venus-arrestins was evaluated using fluorescence at 535 nm upon excitation at 485 nm. Venus-arrestin fluorescence was normalized by the luminescence from the β2AR-RLuc8 to account for variations in cell number and expression. The curves were fit to a sigmoid (BRET ratio) or hyperbola (net BRET) using Prism Version 5.04 (GraphPad Software, San Diego, CA).

Arrestin Interactions with JNK3α2—Venus-arrestin fusions were co-expressed with JNK3α2 fused at the C terminus to RLuc (JNK3α2-RLuc). Forty-eight hours after transfection 5 μM Coelenterazine h was added, and readings were collected by Synergy 4 microplate reader. The BRET signal was determined as the ratio of the light emitted by the Venus-arrestin-3 (528–548 nm) over the light emitted by the JNK3α2-RLuc (460–500 nm). The background signal detected with the ΔN-JNK3α2-RLuc expressed at the same level as JNK3α2-RLuc was subtracted.

Immunofluorescence—COS-7 cells transfected with arrestins, HA-JNK3, and HA-ASK1 were seeded on Lab-Tek chambered slides coated with poly-D-lysine (15 μg/ml) and fibronectin (20 μg/ml) in PBS, serum-starved overnight, washed with PBS, fixed with 4% paraformaldehyde, permeabilized by PBS with 0.2% Triton X-100, and blocked with 3% BSA in PBS for 1 h at room temperature. Venus-arrestin fluorescence was observed directly. Phospho-JNK was detected by indirect immunofluorescence using the phospho-JNK antibody that recognizes all phosphorylated JNK isoforms (Cell Signaling Technology, Inc.) followed by biotinylated anti-mouse IgG (Vector Laboratories) and Alexa Fluor 568 secondary antibody (Molecular Probes). Images were acquired on a Nikon TE2000-E microscope.

Immunoprecipitation—Cells (60 mm plates) were lysed in 0.75 ml of lysis buffer (50 mM Tris, 2 mM EDTA, 250 mM NaCl, 10% glycerol, 0.5% Nonidet P-40, 20 mM NaF, 1 mM sodium orthovanadate, 10 mM *N*-ethylmaleimide, 2 mM benzamide, and 1 mM PMSF) for 30–60 min at 4 °C. After centrifugation, supernatants were precleared by 35 μl of protein G-agarose. Supernatants (250 μg of total protein) were incubated with primary antibodies for 2 h then with 25 μl of protein G-agarose beads for 2 h or overnight. The beads were washed 3 times with 1 ml of lysis buffer, and the proteins were eluted with 50 μl of SDS sample buffer, boiled for 5 min, and analyzed by Western blot (13).

Quantification and Statistical Analysis—The bands on the x-ray film were measured on VersaDoc and quantified using QuantityOne software (Bio-Rad). Statistical significance of the differences between groups was determined using one-way or two-way ANOVA as appropriate followed by Bonferroni/Dunn or Scheffe post hoc tests with correction for multiple comparisons. The details of the analysis of each dataset are given in the figure legends.

RESULTS

Receptor Binding of Structurally Distinct Arrestin-3 Mutants—The first report that arrestin-3 facilitates JNK3 activation implied that this function is associated with the formation of the arrestin-receptor complex (7). Subsequent studies showed that free arrestin-3 and even the $\Delta 7$ mutant, which is impaired in receptor binding (24), effectively promote JNK3 activation (11–14). However, receptor binding of $\Delta 7$ arrestin mutants was only characterized *in vitro* (24), whereas JNK3 activation was measured in living cells (13, 30). Therefore, we used BRET between luciferase-tagged $\beta 2AR$ and Venus-tagged arrestins to compare the ability of several arrestin-3 mutants to bind the receptor in the cellular context (Fig. 1). We recently found that, in contrast to arrestin-2, WT arrestin-3 demonstrates relatively high basal binding to $\beta 2AR$ and that this interaction is enhanced when the receptor is stimulated with a saturating concentration of the agonist isoproterenol (19, 25) (Fig. 1A). The binding difference in the presence and absence of $\beta 2AR$ agonist reaches a maximum at 15 min and then decreases (Fig. 1, A, B, I, and J). In the more flexible arrestin-3-3A (22) the C-tail is detached by a triple alanine substitution of anchoring hydrophobic residues (19) as in the receptor-bound state (32, 33). We confirmed that 3A mutant is even less sensitive to receptor activation, demonstrating the same high binding to active and inactive $\beta 2AR$ that WT arrestin-3 achieves upon agonist stimulation at both time points (Fig. 1, C and D). A seven-residue deletion in the interdomain hinge ($\Delta 7$ mutation) in arrestin-1, -2, and -3 reduces *in vitro* receptor binding by 80–90% (24, 34). We found that in cells receptor binding of $\Delta 7$ is significantly lower than that of WT arrestin-3 or 3A mutant. In this case the difference in binding to active and inactive $\beta 2AR$ was time-dependent; that is, very low at 15 min but increasing to a level comparable to that of WT arrestin-3 by 45 min (Fig. 1, E, F, I, and J). In the case of both WT arrestin-3 and $\Delta 7$ mutant agonist-induced increase of binding saturates at both time points (Fig. 1, I and J). In contrast, KNC mutant, in which 2 key phosphate-binding lysines (25, 35) and 10 residues engaging other receptor elements (18, 25) are substituted with alanines, does not appear to bind active or inactive $\beta 2AR$ at any time point (Fig. 1, G and H). It yields a very low signal comparable to that obtained with free Venus control (supplemental Fig. S1), which apparently reflects nonspecific (usually termed “bystander”) BRET. In contrast, all other forms of arrestin show significantly higher BRET ratios than KNC. Thus, these four forms of arrestin-3 cover a wide range of ability to bind $\beta 2AR$; 3A shows virtually constitutive interaction, basal binding of WT is enhanced by agonist activation, and $\Delta 7$ demonstrates very low basal binding but still interacts with the active receptor, whereas KNC does not bind the receptor at all (Fig. 1). The

binding at both time points that exceeds KNC is shown in Fig. 1K. Complex time-dependent changes in arrestin-receptor interactions were detected in living cells using resonance energy transfer-based methods by others (36). The time course was interpreted as a reflection of multistep interaction: pre-docking followed by binding-induced conformational changes in arrestins (36, 37), with subsequent further changes induced by arrestin interactions with the components of internalization machinery, clathrin, and AP2 (38, 39). Our finding that conformationally constrained $\Delta 7$ mutant shows the most dramatic time dependence (Fig. 1) is consistent with this interpretation.

Biological Activity of Venus-tagged Arrestins and Luciferase-tagged JNK3—Next, we compared the ability of WT and mutant arrestin-3 to facilitate JNK3 phosphorylation. To establish a quantitative *in vivo* arrestin-3-JNK3 interaction assay, we included the same forms of arrestin-3 N-terminal-tagged with Venus, which worked very well in the BRET-based arrestin-receptor interaction assay (18, 19, 25, 40, 41) (Fig. 1). As Venus-tagged forms of arrestin-3 expressed more readily than FLAG-tagged, in these experiments the expression was balanced at the level of FLAG-tagged arrestins by using less plasmids encoding Venus-tagged forms (Fig. 2, A and B). We confirmed previous findings that both WT arrestin-3 and $\Delta 7$ mutant effectively promote JNK3 phosphorylation (12, 13) and found that KNC mutant expressed at the same level was ineffective (Fig. 2, A and B). Very low expression levels of arrestin-3-3A-FLAG did not allow us to compare it to the other FLAG-tagged forms of arrestin-3. N-terminal Venus increased the expression of all forms of arrestin-3, including 3A mutant, which allowed functional comparison of all four forms of arrestin-3 at higher expression level (Fig. 2, C and D). Venus-tagged arrestins activate JNK at least as efficiently as the corresponding forms with the C-terminal FLAG tag (Fig. 2, A and B). Importantly, WT arrestin-3 and $\Delta 7$ mutant comparably activate JNK3 in both FLAG- and Venus-tagged forms, whereas 3A and KNC are essentially inactive (Fig. 2). Thus, the N-terminal Venus tag does not change the relative ability of different forms of arrestin-3 to promote JNK3 phosphorylation, which makes them adequate tools for measuring biologically relevant interactions between arrestin-3 and its binding partners *in vivo*.

Because an *in vivo* interaction assay requires tagging of both partners, next we tested whether JNK3 $\alpha 2$ C-terminal-tagged with luciferase (JNK3-Luc) can be activated in cells expressing ASK1 and arrestin-3. We found that JNK3-Luc phosphorylation in the cell was arrestin-3-dependent, similar to HA-tagged JNK3 (Fig. 2, E and F). Thus, neither N-terminal Venus tag on arrestin-3 nor C-terminal luciferase tag on JNK3 significantly affects their biologically relevant interaction in the cell that results in JNK3 activation (Fig. 2). This makes these fusion proteins appropriate tools for measuring arrestin-3 interactions with JNK3 by BRET in living cells.

Mutations in Arrestin-3 Differentially Affect Its Interaction with JNK3 in Living Cells—The major limitation of energy transfer-based interaction assays in living cells is nonspecific BRET or FRET (42, 43), which needs to be measured and subtracted to determine specific signal. Although free fluorescent proteins and/or luciferase can be used for this purpose, these proteins are much smaller than their fusions with proteins of

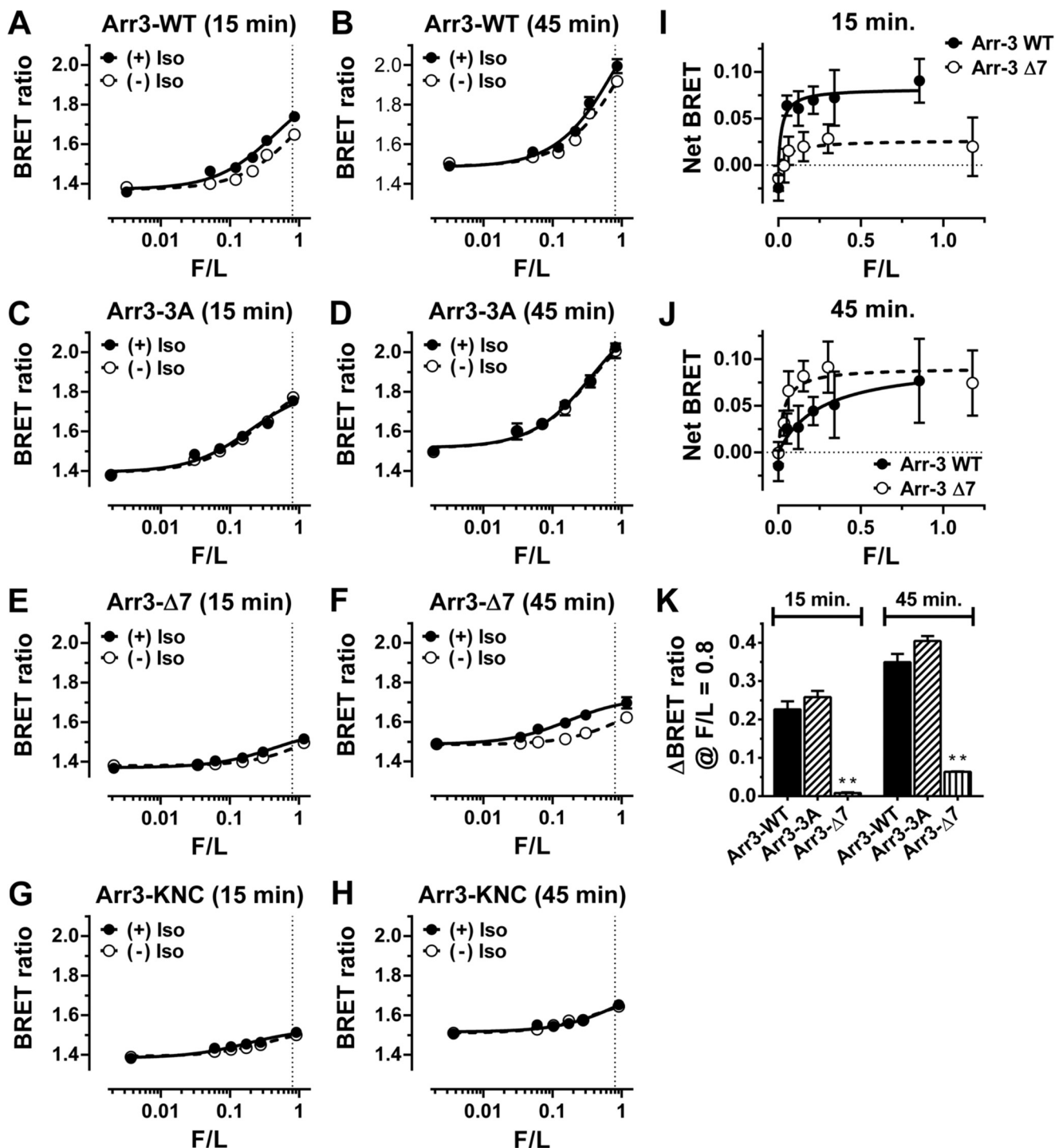


FIGURE 1. Receptor binding characteristics of arrestin-3 mutants. A–H, N-terminal Venus-tagged WT arrestin-3 (*Arr3*) (A and B), arrestin-3-3A (3A) (C and D), arrestin-3-Δ7 (Δ7) (E and F), or arrestin-3-KNC (*KNC*) (G and H) were expressed with β_2 AR tagged with C-terminal *Renilla* luciferase variant 8 (β_2 AR-RLuc8). BRET ratios in the presence of β -agonist isoproterenol ((+) Iso; filled symbols) or vehicle (–) Iso; open symbols) as a function of the expression of indicated arrestins are shown at 15 min (A, C, E, and G) and 45 min (B, D, F, and H) after the addition of luciferase substrate. The means \pm S.D. of six parallel measurements in a representative experiment (of two to four performed for each form of arrestin-3) are shown. F/L, fluorescence/luminescence ratio, which reflects the expression ratio of Venus-arrestins and β_2 AR-RLuc8. I and J, shown is net BRET (a difference between BRET ratios in the presence and absence of agonist) between WT or Δ7 arrestin-3 and β_2 AR-RLuc8 at 15 min (I) and 45 min (J) after the addition of luciferase substrate. K, specific arrestin-receptor BRET is shown. The BRET signal obtained with KNC mutant (which was not significantly different from that obtained with free Venus and, therefore, considered nonspecific; see supplemental Fig. S1) was subtracted from BRET ratios obtained in the presence of isoproterenol with the indicated mutants at 15 and 45 min (means \pm S.D. of three independent experiments). The data were analyzed by one-way ANOVA with protein as a main factor. **, $p < 0.01$, as compared with WT arrestin-3.

interest and, therefore, can diffuse faster. The best possible control in these cases is the same fusion protein with mutations that preclude specific interaction. The deletion of 39 N-termi-

nal JNK3 residues (Δ N-JNK3) was shown to abolish its binding to both non-visual arrestins (12, 44). Indeed, Venus-arrestin-3 demonstrates higher levels of BRET with JNK3-Luc than with

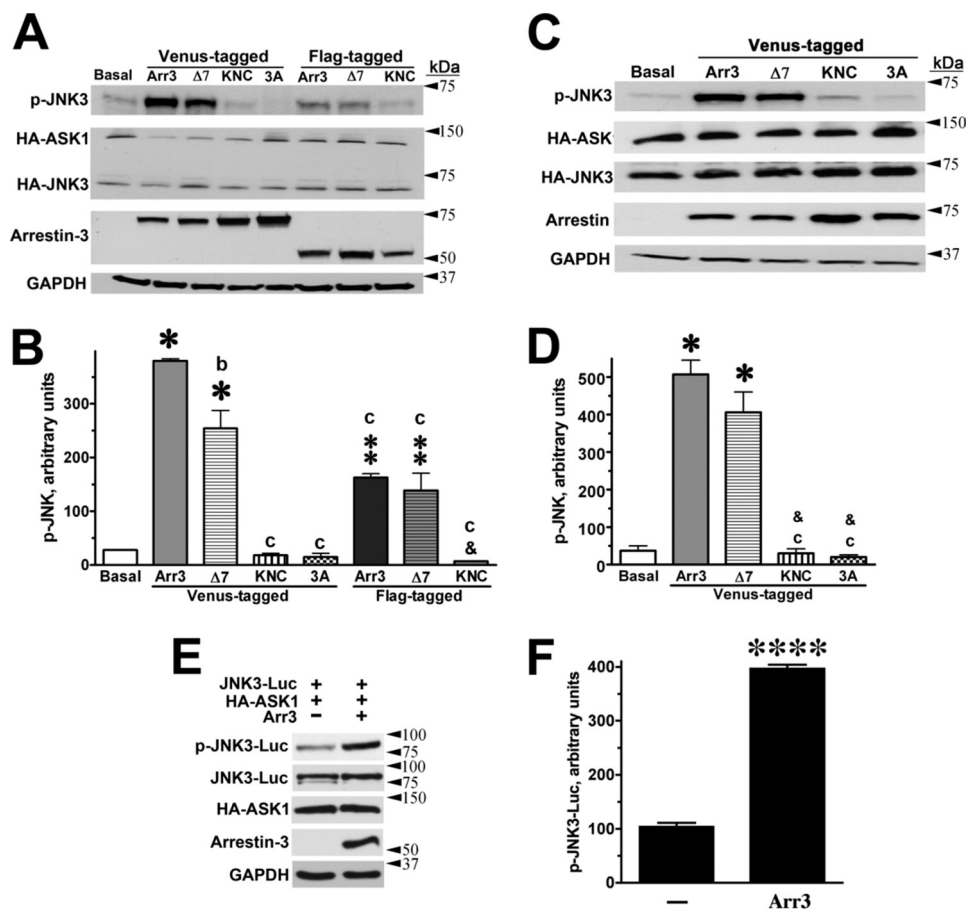


FIGURE 2. Venus tag on arrestin-3 and luciferase tag on JNK3 does not significantly affect arrestin-dependent JNK3 activation. *A*, COS-7 cells were transfected with HA-ASK1, HA-JNK3, and the indicated arrestins with C-terminal FLAG tag or N-terminal Venus tag, harvested in 48 h, and lysed. The amounts of active phosphorylated JNK3 (*top blot*, p-JNK3) and the expression of ASK1, JNK3, and arrestins were determined by Western blot. The results of a representative experiment of four performed are shown. *Arrowheads on the right* indicate the positions of molecular mass markers. *B*, shown is quantification of the level of JNK3 phosphorylation (the intensity of p-JNK3 bands shown in *A*) in cells expressing the indicated arrestins in four independent experiments. The data were analyzed by one-way ANOVA with protein (basal with no extra arrestin, WT, or indicated mutants with different tags) as a main factor. The effect of protein was highly significant ($F(7,16) = 64.1, p < 0.001$). *, $p < 0.001$; **, $p < 0.01$ to basal; *c*, $p < 0.001$; *b*, $p < 0.01$ to Venus-WT; &, $p < 0.001$ to WT-FLAG, according to Bonferroni/Dun post hoc test with correction for multiple comparisons. *C*, direct comparison of the ability of Venus-tagged forms of arrestin-3 to promote JNK3 phosphorylation is shown. The experiments were performed, and the data are presented as in *panel A*. *D*, quantification of the intensity of p-JNK3 bands in three experiments (shown in *C*) is shown. The data were analyzed by one-way ANOVA with protein as a main factor, as in *B*. The effect of protein was highly significant [$F(4,15) = 60.2, p < 0.001$]. *, $p < 0.001$; **, $p < 0.01$ to basal; *c*, $p < 0.001$ to Venus-arrestin-3 (WT); &, $p < 0.001$ to Venus-arrestin-3-Δ7, according to Bonferroni/Dunn post hoc test with correction for multiple comparisons. *E*, COS-7 cells transfected with HA-ASK1 and JNK3-Luc with or without WT arrestin-3 were harvested in 48 h and lysed. The amounts of active phosphorylated JNK3-Luc (*top blot*, p-JNK3-Luc) and the expression of ASK1, JNK3-Luc, and arrestin-3 were determined by Western blot. The results of a representative experiment of three performed are shown. *Arrowheads on the right* indicate the positions of molecular mass markers. *F*, quantification of the level of JNK3-Luc phosphorylation (the intensity of p-JNK3-Luc bands shown in *E*) in cells that do (Arr3) or do not (–) express arrestin-3 in three independent experiments. ****, $p < 0.0001$ to control.

ΔN-JNK3-Luc (Fig. 3A). Free luciferase, ΔN-JNK3-luc, and Venus-tagged arrestin-3-Δ7 showed the same level of BRET (Fig. 3B), suggesting that it is exclusively nonspecific. Moreover, ΔN-JNK3 phosphorylation was not enhanced by arrestin-3, WT, or Δ7, both of which robustly increased phosphorylation of full-length JNK3 under the same conditions (Fig. 3, E and F). These results show that ΔN-JNK3 does not specifically interact with arrestin-3, establishing it as an appropriate control for nonspecific BRET.

Therefore, we used BRET between JNK3-luciferase and different forms of Venus-tagged arrestin-3 as a quantitative measure of their interactions in native cell milieu, subtracting nonspecific BRET between ΔN-JNK3-luciferase and the same forms of arrestin-3 in each case (Fig. 3, C and D). Unexpectedly, we found that JNK3-luciferase yields significant, but fairly low BRET with WT arrestin-3 and 3A mutant, whereas KNC and

Δ7 forms of arrestin-3 yielded 2–3-fold higher BRET signal (Fig. 3, C and D). Thus, all four forms of arrestin-3 specifically bind JNK3. However, WT arrestin-3 and Δ7 mutant, which facilitates JNK3 phosphorylation equally well (Figs. 2, A–D, and 3, E and F), demonstrate a dramatic difference in JNK3 binding (Fig. 3, C and D). The two inactive forms, KNC and 3A, also significantly differ in their ability to bind JNK3 (Figs. 2 and 3). Interestingly, completely inactive KNC mutant appears to bind JNK3 better than WT arrestin-3, which promotes robust JNK3 phosphorylation (Figs. 2 and 3). The strength of the BRET signal between two proteins reflects both their proximity and relative orientation of luciferase and Venus tags. Thus, one possible interpretation of stronger BRET between JNK3-Luc and arrestin-3-Δ7 could be that the orientation of Venus fused to this conformationally restricted mutant (24) is more favorable, whereas the orientation of Venus fused to conformationally

JNK Inhibition by Silent Scaffold

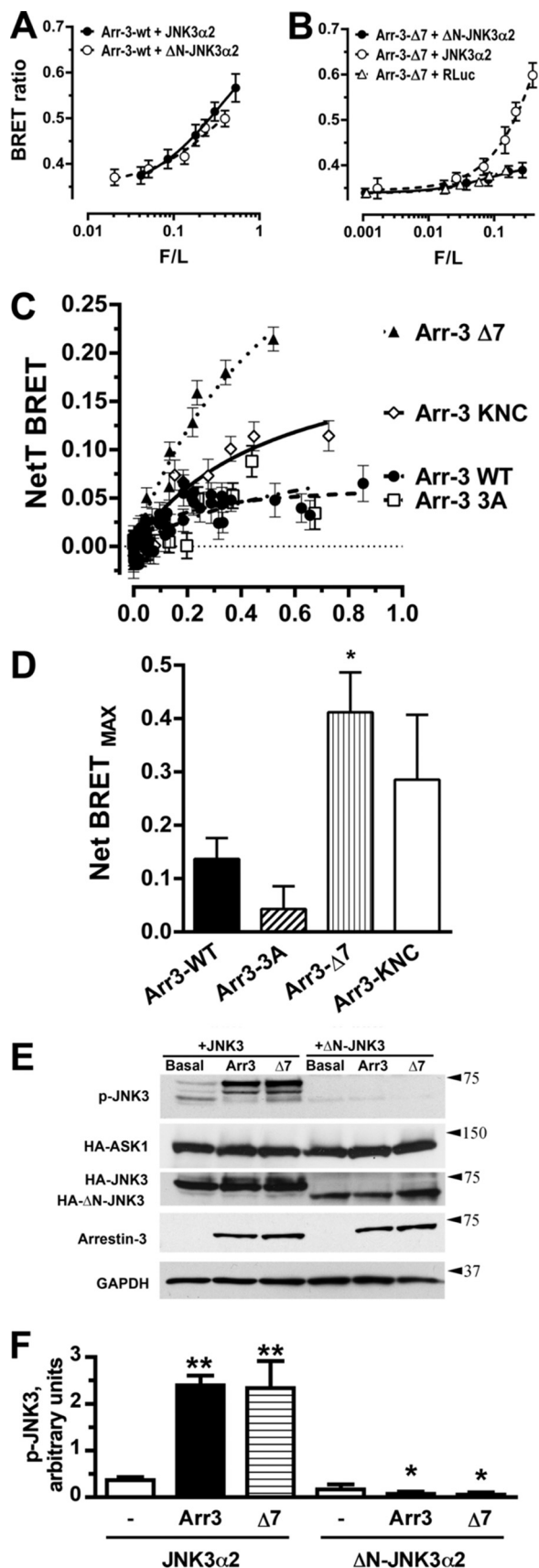


FIGURE 3. Differential interaction of arrestin-3 mutants with JNK3. A, increasing amounts of Venus-arrestin-3 were expressed with JNK3 α 2-RLuc and Δ N-JNK3 α 2-RLuc. BRET ratios as a function of arrestin-3 expression in a

representative experiment (of three performed) are shown. B, increasing amounts of Venus-arrestin-3- Δ 7 were expressed with JNK3 α 2-RLuc, Δ N-JNK3 α 2-RLuc, or free *Renilla* luciferase variant 8 (RLuc). BRET ratios as a function of arrestin-3- Δ 7 expression in a representative experiment (of three performed) are shown. Note that the BRET ratios obtained with RLuc and Δ N-JNK3 α 2-RLuc are virtually identical, indicating that the signal with JNK3 α 2-(Δ 2–39)-RLuc is nonspecific. C, increasing amounts of Venus-tagged WT arrestin-3 (Arr-3), arrestin-3-3A (3A), arrestin-3- Δ 7 (Δ 7), or arrestin-3-KNC (KNC) were expressed with a fixed amount of JNK3 α 2-RLuc. Net BRET (BRET ratio with JNK3 α 2-RLuc minus ratio with Δ N-JNK3 α 2-RLuc) as a function of arrestin expression in a representative experiment (of three performed) is shown. D, quantification of BRET max between full-length JNK3 α 2-RLuc and indicated Venus-tagged forms of arrestin-3. The data were analyzed by one-way ANOVA with protein (WT or mutant arrestin-3) as a main factor. The effect of protein was significant [F(3,10) = 4.67, p = 0.0274]. *, p < 0.05 to WT and 3A (Bonferroni/Dunn post hoc test). E, COS-7 cells were transfected with HA-ASK1, HA-JNK3, or HA- Δ N-JNK3 and the indicated Venus-tagged arrestins, harvested in 48 h, and lysed. The amounts of active phosphorylated JNK3 (*top blot*, p-JNK3) and the expression of ASK1, JNK3, and arrestins were determined by Western blot. The results of a representative experiment are shown. Arrowheads on the right indicate the positions of molecular mass markers. F, quantification of JNK3 phosphorylation in three experiments is shown. The data were analyzed by two-way ANOVA with arrestin (no arrestin, arrestin-3, arrestin-3- Δ 7) and JNK3 (JNK3 versus Δ N-JNK3) as main factors. The effects of both factors were significant as well as the arrestin \times JNK3 interaction (p < 0.0001). The significant effect of the JNK3 factor indicates that the level of Δ N-JNK3 phosphorylation was significantly lower than that of WT JNK3 in all conditions regardless of the co-expression of arrestin proteins. Separate analysis of the activation of WT JNK3 revealed significant effect of arrestin (F(2,6) = 31.0, p = 0.0007), with both arrestin-3 and arrestin-3- Δ 7 significantly increasing JNK3 activity as compared with the basal condition: **, p < 0.01 to basal (–) according to Bonferroni/Dunn post hoc test. Note that in contrast to HA-JNK3, the phosphorylation of HA- Δ N-JNK3 is not affected by arrestin-3 (p = 0.24).

loose arrestin-3-3A (22) is less favorable for energy transfer. Although we cannot rule out this possibility, the fact that KNC mutant with normal conformational flexibility also shows more efficient BRET with JNK3-Luc suggests that the relative strength of the interaction of different forms of arrestin-3 with JNK3 contributes to the observed differences in BRET signal.

Ability of Arrestin-3 Mutants to Promote JNK3 Activation and Subcellular Localization of Active JNK3 Is Not Affected by Receptor—The original report suggested that the receptor-arrestin complex acts as a scaffold for the ASK1-MKK4-JNK3 cascade (7), although subsequent studies indicated that free arrestin-3 can perform this function (11–14). Full activity of receptor binding-impaired Δ 7 mutant (24) was considered the strongest argument against the role of G protein-coupled receptors in JNK3 activation (12). However, our cell-based assay revealed that although arrestin-3- Δ 7 did not show any appreciable basal interaction with β 2AR, agonist stimulation promoted a slow increase in specific binding of Δ 7 mutant to the receptor (Fig. 1, E, F, I, J, and K). Although agonist activation of β 2AR can promote MAPK activation via G protein-mediated signaling (45), the binding of the biased agonist ICI118551, which acts as an inverse agonist for G protein coupling, selectively facilitates arrestin-mediated signaling to MAPKs (27, 28, 46). To test whether receptor binding plays any role in JNK3 activation, we transfected COS-7 cells with different forms of arrestin-3, JNK3, and ASK1, activated endogenous β 2AR with the classical agonist isoproterenol or ICI118551, and measured the levels of phosphorylation of ERK1/2, which is known to be specifically activated by the receptor-bound arrestin (28, 46) and of JNK3 in the same cells (Fig. 4). The data revealed a robust increase in ERK1/2 phosphorylation in response to endogenous

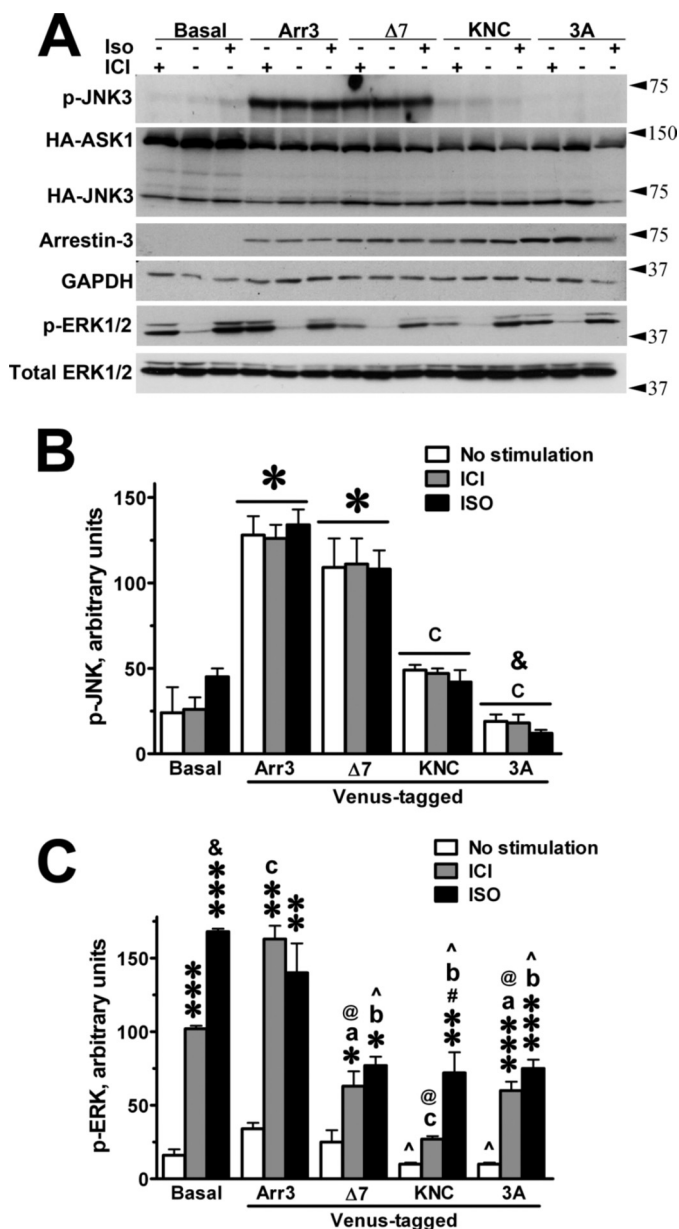


FIGURE 4. Arrestin-dependent increase in JNK3 phosphorylation is not affected by receptor activation, in contrast to ERK1/2 phosphorylation in the same cells. *A*, COS-7 cells were transfected with HA-ASK1, HA-JNK3, and the indicated Venus-tagged arrestins. Cells were serum-starved overnight and treated for 8 min at 37 °C with vehicle, 10 μ M β 2AR agonist isoproterenol (*Iso*), or 1 μ M ICI118551 (*ICI*), which is an inverse agonist for G proteins and biased agonist for arrestins, to activate endogenous β 2AR. Cells were then harvested and lysed. The amounts of active phosphorylated JNK3 (*p-JNK3*), the expression of ASK1, JNK3, and arrestins as well as total and phosphorylated endogenous ERK1/2 were determined by Western blot. The results of a representative experiment of three performed are shown. *Arrowheads on the right* indicate the positions of molecular mass markers. *B*, quantification of JNK3 phosphorylation (the intensity of *p-JNK3* bands) is shown. The data were analyzed by two-way ANOVA with protein (basal with no extra arrestin, WT, or mutant arrestins) and treatment (vehicle versus *ICI* or *Iso*) as main factors. The effect of protein was highly significant [$F(4,30) = 85.3, p < 0.001$], whereas neither the effect of treatment nor protein \times treatment interaction was significant ($p > 0.8$). $*$, $p < 0.001$ to basal; $c, p < 0.001$ to WT and $\Delta 7$; $\&, p < 0.01$ to KNC for the protein effect according to Bonferroni/Dunn post hoc test with correction for multiple comparisons. *C*, shown is quantification of endogenous ERK1/2 phosphorylation (the intensity of *p-ERK1/2* bands). The data were analyzed by two-way ANOVA with protein (basal with no extra arrestin, WT, or mutant arrestins) and treatment (vehicle versus *ICI* or *Iso*) as main factors. The effects of both factors were highly significant ($F(4,30) = 47.7, p < 0.001$, and $F(2,30) = 154.1, p < 0.0001$, for protein and treatment,

β 2AR stimulation with isoproterenol or ICI118551 in control COS-7 cells containing endogenous levels of arrestins and in cells overexpressing WT arrestin-3. The expression of $\Delta 7$, KNC, or 3A mutants reduced ERK1/2 phosphorylation, particularly in response to ICI118551 stimulation (Fig. 4, *A* and *C*), suggesting that these forms of arrestin-3 act as dominant suppressors of receptor-mediated ERK1/2 activation. We previously found that two of three kinases in cRaf-1-MEK1-ERK1/2 cascade are sensitive to arrestin conformation, whereas MEK1 is not (28). We also found that, in contrast to WT arrestin-3, 3A and $\Delta 7$ mutants associate with ERK1/2 independently of receptor binding (28). Thus, the mechanism of the suppression of ERK1/2 activity by $\Delta 7$, KNC, and 3A mutants is likely similar to the mechanism underlying dominant-negative action of KNC in JNK cascade; that is, recruitment of kinases into unproductive complexes. Importantly, WT arrestin-3 and $\Delta 7$ mutant significantly increased the level of JNK3 phosphorylation, whereas KNC and 3A mutants did not. In all cases we did not detect any effect of receptor stimulation on JNK3 activation (Fig. 4, *A* and *B*). Thus, arrestin-3-dependent JNK3 activation does not appear to be regulated by receptor activity in any way in cells that clearly respond to receptor stimulation by arrestin-biased agonist with significant changes in ERK1/2 phosphorylation.

JNK3, particularly in its active phosphorylated form, tends to localize to the nucleus (12, 15, 17, 47). Interestingly, JNK3 activated via arrestin-3-mediated mechanism was reported to remain in the cytoplasm, presumably due to cytoplasmic localization of receptor-bound arrestin-3 (7). However, arrestin-3 has a functional nuclear export signal in the C terminus (17, 47) that was shown to determine the cytoplasmic localization of arrestin-3 itself and even its interaction partners that normally localize to the nucleus, such as JNK3 or ubiquitin ligase Mdm2 (15, 17, 47). Our data show that arrestin-3 facilitates the activation of JNK3 independently of receptors (Fig. 4) and that only two arrestin-3 forms tested promote JNK3 activation (Figs. 2, 3, and 4). Therefore, we used immunocytochemistry to determine the localization of different forms of arrestin-3 and phosphorylated JNK in COS-7 cells (Fig. 5). We found that WT arrestin-3 and all mutants remain virtually exclusively cytoplasmic, as could be expected based on the fact that they all retain functional nuclear export signal. Interestingly, in cells expressing WT arrestin-3 and $\Delta 7$ mutant, both of which robustly facilitate JNK3 activation (Figs. 2, 3, and 4), the majority of phosphorylated JNK was found in the cytoplasm (Fig. 5). In contrast, in cells expressing KNC or 3A mutants, where JNK3 activation can only occur via arrestin-independent mechanisms, most of the phospho-JNK was detected in the nucleus (Fig. 5). Taken together, these data support the idea that JNK3 activated with

respectively). The protein \times treatment interaction was also highly significant ($F(8,30) = 12, p < 0.0001$), suggesting that receptor stimulation differentially affected ERK phosphorylation in the presence of different forms of arrestin-3. Means were compared using Bonferroni/Dunn post hoc test with corrections for multiple comparisons after one-way ANOVA with treatment as the main factor performed separately for control and for each protein. $***, p < 0.001$; $** , p < 0.01$; $* , p < 0.05$ to vehicle; $\&, p < 0.01$ to ICI. Alternatively, comparison of means was made with Bonferroni/Dunn post hoc test after one-way ANOVA with protein as a main factor performed separately for each treatment condition. *a, p < 0.05*; *b, p < 0.01*; *c, p < 0.001* to CO; $\wedge, p < 0.05$; $\wedge , p < 0.001$ to WT.

JNK Inhibition by Silent Scaffold

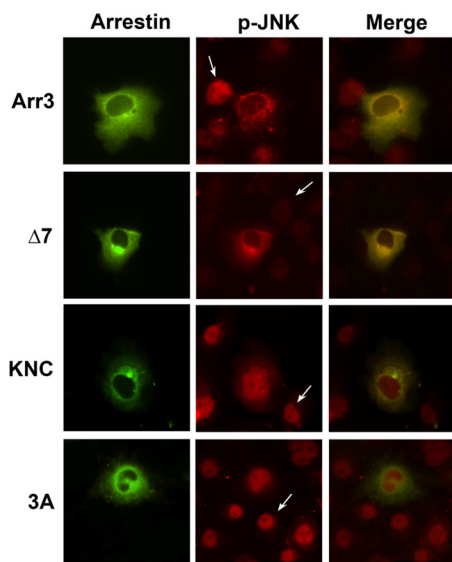


FIGURE 5. Cytoplasmic localization of JNK activated via arrestin-dependent mechanism. COS-7 cells transfected with HA-JNK3, HA-ASK1, and the indicated arrestins were seeded on Lab-Tek chambered slides, serum-starved overnight, washed with PBS, and fixed with 4% paraformaldehyde. Venus-arrestin fluorescence was observed directly (arrestin, green). Phospho-JNK was detected by indirect immunofluorescence using the phospho-JNK antibody and Alexa Fluor 568-conjugated secondary antibody (*p*-JNK, red). Single-channel and merged images were acquired on a Nikon TE2000-E microscope. Note that all forms of arrestin-3 are cytoplasmic, whereas active JNK is predominantly cytoplasmic in cells expressing WT arrestin-3 and $\Delta 7$ mutant. The arrows in the *p*-JNK column indicate cells that do not express arrestins, where *p*-JNK (likely activated endogenous JNK1 and JNK2 isoforms) invariably localizes to the nucleus. Representative cells are shown.

the help of arrestin-3 remains cytoplasmic and demonstrate that receptor binding of arrestin-3 does not play any role in this localization. In fact, one of the two active forms of arrestin-3 (WT) and one of the completely inactive ones (3A) in JNK3 activation assay robustly bind $\beta 2$ AR (Fig. 1), whereas the other equally effective JNK3 activator ($\Delta 7$) and the second inactive form (KNC) are significantly impaired in receptor binding (Fig. 1). Thus, the cytoplasmic localization of arrestin-3 drives co-localization of JNK3 activated via arrestin-dependent mechanism to the cytoplasm.

Most non-neuronal cells, including COS-7, endogenously express several isoforms of JNK1 and JNK2. Because anti-phospho-JNK antibody recognizes all isoforms of phosphorylated JNK equally, it is likely that nuclear phospho-JNK observed (Fig. 5) represents endogenous JNK1 and JNK2 activated via non-arrestin scaffolds. Because all forms of arrestin-3 have functional nuclear export signal (15, 17, 47) and remain predominantly in the cytoplasm (Fig. 5), it is hardly surprising that even dominant-negative KNC cannot compete with nuclear scaffolds and suppress JNK phosphorylation in this compartment. It is also worth noting that standard buffers used to lyse cells for Western blotting (Figs. 2, 3, 4, and 6) or immunoprecipitation (Fig. 6) do not lyse nuclei, which are, therefore, lost along with cell debris. These experimental paradigms are suitable for the detection of JNK activity in the cytoplasm, but not in the nucleus, which explains the absence of phospho-JNK signal on Westerns blots (Figs. 2, 3, 4, and 6). The combination of these approaches with immunocytochemistry (Fig. 5) is necessary to fully characterize the activity of any MAP kinase in cells.

Arrestin-3-KNC Mutant Binds ASK1, MKK4, and JNK3 and Effectively Suppresses JNK3 Activation—Our data demonstrate that the KNC mutant binds JNK3 better than WT arrestin-3 (Fig. 3) yet does not have the ability to promote JNK3 activation (Figs. 2, 3, and 4). These results suggest that the KNC mutant can sequester JNK3 away from arrestin-3 and other scaffolds that facilitate its phosphorylation, a combination of characteristics necessary for dominant-negative function. To test this idea, we co-expressed WT arrestin-3 with different amounts of KNC mutant (Fig. 6A). To enable direct comparison of the expression level of both proteins on the same blot, we used FLAG-tagged WT arrestin-3 and Venus-tagged KNC with distinctly different electrophoretic mobility (Fig. 6A). We found that increasing expression of KNC mutant progressively decreases JNK3 phosphorylation, virtually eliminating the effect of arrestin-3 at $\sim 2:1$ molar ratio (Fig. 6, A and B). These data suggest that the KNC mutant inhibits JNK3 phosphorylation by competing with WT arrestin-3. We found an essentially linear correlation between KNC expression and the inhibition of JNK3 phosphorylation ($R^2 = 0.8611$; $p < 0.0001$) (Fig. 6C). Thus, the KNC mutant is an effective suppressor of JNK3 activation, which makes it the first dominant-negative form of arrestin-3 in this regard.

Two molecular mechanisms can explain the dominant-negative action of the KNC mutant; the binding to JNK3 without engaging upstream kinases or the interaction with all three kinases in the ASK1-MKK4-JNK3 module and assembling the complex in the “wrong” way, thereby making it unproductive. To determine the mechanism of this dominant-negative function, we expressed Venus-tagged WT, $\Delta 7$, KNC, and 3A forms of arrestin-3 along with HA-tagged ASK1, MKK4, and JNK3, immunoprecipitated arrestins with anti-GFP antibody and then quantified each kinase in the complex by Western blot (Fig. 6, D–H). We found that $\Delta 7$ binds all kinases better than WT arrestin-3, whereas the KNC mutation enhances arrestin-3 interaction with JNK3 and does not appreciably change its ability to bind ASK1 and MKK4 (Fig. 6, D–G). These results support the idea that enhanced BRET between the KNC mutant and JNK3 (Fig. 3, C and D) reflects higher affinity of the interaction than with WT arrestin-3. Despite enhanced interactions, $\Delta 7$ mutant facilitates JNK3 activation less efficiently than WT arrestin-3 (Figs. 2 and 6I). However, tighter binding translates into higher levels of active *p*-JNK3 associated with $\Delta 7$ than with WT arrestin-3 (Fig. 6H), in agreement with very efficient localization of *p*-JNK to the cytoplasm by this mutant (Fig. 5). Due to enhanced binding, more JNK3 associates with KNC than with WT arrestin-3, but all of it remains inactive (Fig. 6, D, E, and H). Because KNC mutant binds ASK1 and MKK4 as well as WT arrestin-3 and JNK3 even better (Fig. 6, E, F, and G), it apparently reduces JNK3 activation by sequestering all three kinases in unproductive complexes (Fig. 6I). This mechanism makes it an even more powerful dominant suppressor of JNK activity than it would have been if it interacted only with JNK3.

DISCUSSION

The participation of non-visual arrestins in the regulation of JNK3 activity was discovered more than a decade ago (7). However, surprisingly few mechanistic details of this process have

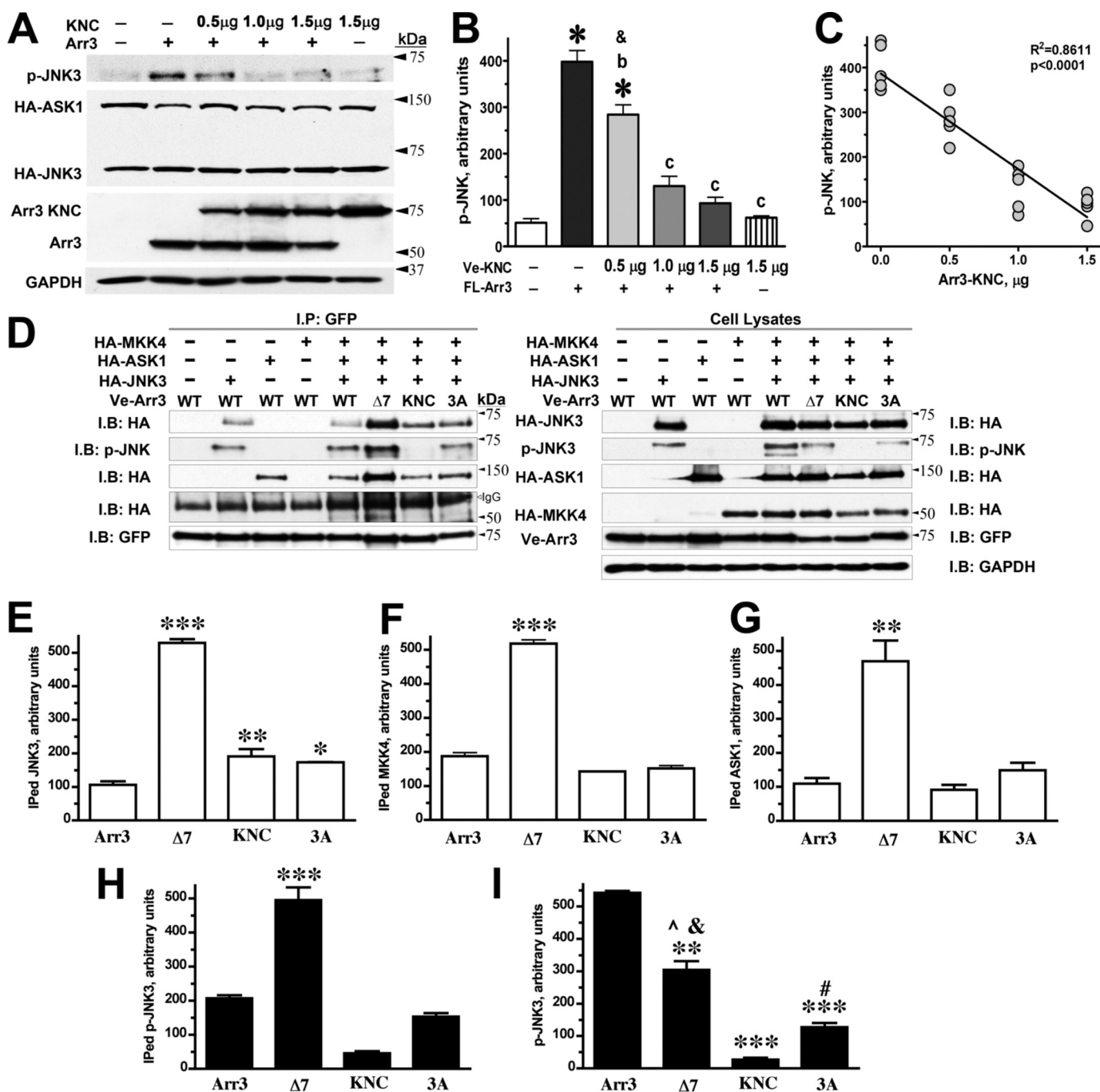


FIGURE 6. Dominant-negative action of silent scaffold arrestin-3-KNC. *A*, COS-7 cells were transfected with HA-ASK1, HA-JNK3, and the same amount of WT arrestin-3-FLAG (Arr3-WT) and the indicated amounts of Venus-arrestin-3-KNC, harvested 48 h after transfection, and lysed. The amounts of active phosphorylated JNK3 (top blot, p-JNK3) and the expression of ASK1, JNK3, and arrestins were determined by Western blot. The results of a representative experiment of five were performed as shown. Arrowheads on the right indicate the positions of molecular mass markers. *B*, shown is quantification of the level of JNK3 phosphorylation (the intensity of p-JNK3 bands shown in *A*) in cells expressing the indicated arrestins in three independent experiments. The data were analyzed by one-way ANOVA with protein (basal with no extra arrestin, WT arrestin-3-FLAG (FL-Arr3) without and with increasing concentrations of Venus-KNC (Ve-KNC) or Venus-KNC alone) as the main factor. The effect of protein was highly significant [$F(5,24) = 67.8, p < 0.001$]. *, $p < 0.001$ to basal; b, $p < 0.01$; c, $p < 0.001$ to WT arrestin-3-FLAG; &, $p < 0.001$ to Venus-KNC (Bonferroni/Dunn post hoc test with correction for multiple comparisons). *C*, a linear regression model with a Venus-KNC DNA amount (in μg) as an independent variable yielded significant $F(1,19) = 111.6, p < 0.0001$ and adjusted $R^2 = 0.8611$, indicating progressive inhibition of JNK3 activation by increasing amounts of arrestin-3-KNC acting as a dominant-negative silent scaffold. *D*, COS-7 cells were transfected with the indicated HA-tagged kinases and Venus-tagged arrestins and lysed 48 h after transfection, and arrestins were immunoprecipitated with anti-GFP antibody. The expression of all proteins and amounts of active phosphorylated JNK3 (p-JNK3) in the lysate (right panel, Cell lysates) and in the immunoprecipitate (left panel, IP:GFP) were determined by Western blot (I.B.). The results of a representative experiment are shown. Arrowheads on the right indicate the positions of molecular mass markers. *E–I*, the amounts of co-immunoprecipitated HA-JNK3 (*E*), MKK4 (*F*), ASK1 (*G*), phosphorylated JNK3 (p-JNK3) (*H*), and active p-JNK3 in cell lysate (*I*) in two experiments were determined and statistically analyzed using ANOVA with arrestin as the main factor followed by post-hoc Scheffe test. Statistical significance of the differences is indicated as follows: *E*, ***, $p < 0.001$ to Arr3, KNC, and 3A; **, $p < 0.01$; *, $p < 0.05$ to WT arrestin-3 (Arr3); *F*, ***, $p < 0.001$ to Arr3, KNC, and 3A; *G*, **, $p < 0.01$ to Arr3, KNC, and 3A; *H*, ***, $p < 0.01$ to Arr3 and $p < 0.001$ to KNC; *I*, ***, $p < 0.001$ and **, $p < 0.01$ to Arr3; &, $p < 0.01$ to KNC; ^, $p < 0.01$ to 3A; #, $p < 0.05$ to KNC.

JNK Inhibition by Silent Scaffold

been unambiguously elucidated. One controversial issue was the role of receptor binding. The first report suggested that receptor-bound arrestin-3 facilitates JNK3 activation (7), whereas subsequent studies from the same group (11) and others (12) showed that free arrestin-3 is capable of performing this function. A recent demonstration that arrestin-3 scaffolding of the MKK4-JNK3 module can be reproduced with purified proteins in the absence of receptors (14) definitively proved this idea. Here we used four forms of arrestin-3, two of which robustly bind β 2AR, whereas the other two are significantly impaired in receptor binding in the environment of an intact cell (Fig. 1). We found that each category contains one form of arrestin-3 that effectively promotes JNK3 phosphorylation and another form that was completely inactive in this regard (Fig. 2). WT arrestin-3 facilitates ERK1/2 phosphorylation in response to β 2AR stimulation by isoproterenol and ICI118551, whereas Δ 7 mutant does not (Fig. 4). In the same cells both forms of arrestin-3 facilitate JNK3 activation equally effectively, and the level of JNK3 phosphorylation is unaffected by receptor ligands (Fig. 4). These data unambiguously demonstrate that receptor binding and JNK3 activation are independent functions of arrestin-3 that can be separately manipulated by mutagenesis without necessarily affecting each other.

JNK3 activated via conventional mechanisms localizes to the nucleus (48), where it phosphorylates various transcription factors, changing mRNA synthesis (49). We confirmed a previous report (7) that JNK3 activated by an arrestin-dependent mechanism behaves differently and remains in the cytoplasm (Fig. 5). We confirmed cytoplasmic localization of phospho-JNK3 activated via WT arrestin-3 that robustly binds receptors. Importantly, JNK3 phosphorylated with the help of Δ 7 mutant with significantly impaired receptor binding ability also remains in the cytoplasm (Fig. 5). Moreover, we found that in the presence of arrestin-3-3A, which binds β 2AR even more readily than WT (Fig. 1) and interacts with JNK3 with essentially the same affinity (Figs. 3 and 6) but fails to promote JNK3 activation (Figs. 2 and 4), the majority of phospho-JNK (likely representing endogenous JNK1 and JNK2 isoforms) is found in the nucleus (Fig. 5). These data show that only phospho-JNK3 activated via arrestin-3 is retained in the cytoplasm. This localization does not appear to depend on arrestin-3 binding to the receptor but is likely determined by the cytoplasmic localization of arrestin-3 itself due to the presence of a functional nuclear export sequence in its C terminus (17, 47).

Arrestin-3 interaction with JNK3 in cells was detected by co-immunoprecipitation (7, 13, 44) or nuclear exclusion of JNK3 (12, 15, 17). Although these data show that arrestin-3 and JNK3 are in the same macromolecular complex, neither assay can prove that these two proteins interact directly or via unknown intermediate(s). Moreover, both are essentially threshold "yes-or-no" assays that cannot be used for quantitative comparison of the ability of different forms of arrestin-3 to bind JNK3. Therefore, we established a novel cell-based assay where the interaction is detected as BRET signal between luciferase-tagged JNK3 and Venus-tagged arrestin. Although even this method does not definitively prove direct interaction, distance limitations for effective energy transfer (50, 51) strongly suggest that arrestin-3 directly binds JNK3. One of the limita-

tions of BRET- and FRET-based interaction assays is that the efficiency of energy transfer depends on the relative orientation of luciferase and/or fluorescent protein, which can affect the signal as much as the distance between the two moieties. Although the difference between flexible WT arrestin-3 (19) and conformationally restrained Δ 7 mutant (24) could have contributed to the observed difference in BRET efficiency (Fig. 3, C and D), crystal structures of all vertebrate arrestins (19, 52–54) suggest that KNC mutant likely retains the conformational flexibility of the parental protein. This BRET-based assay is more quantitative than any used so far for this interaction, allowing us to show that WT arrestin-3 and 3A mutant comparably bind JNK3, whereas JNK3 interactions with KNC and especially Δ 7 mutant are significantly stronger (Fig. 3). It is noteworthy that the nuclear exclusion assay failed to detect considerable differences in JNK3 binding of WT arrestin-3 and its 3A or Δ 7 mutants (15), which was clearly revealed by BRET (Fig. 3) and co-immunoprecipitation (Fig. 6). Importantly, these data along with the comparison of JNK3 phosphorylation in cells expressing different forms of arrestin-3 (Figs. 2, 3, 4, and 6) demonstrate that the strength of JNK3 binding does not correlate with the ability of arrestin-3 to promote JNK3 activation.

MAPK activity in the cell is organized by scaffolding proteins, which arrange appropriate combinations of kinases into productive signaling modules (55, 56). Our discovery that KNC mutant binds JNK3 better than WT protein (Fig. 3) and interacts with upstream kinases ASK1 and MKK4 normally (Fig. 6) yet does not facilitate JNK3 activation (Figs. 2, 3, 4, and 6) opens the possibility to manipulate JNK3 signaling in a novel way that was not previously explored. This combination of functional characteristics suggests that KNC mutant has a potential to act as a silent scaffold, scavenging JNK3 away from productive scaffolds that could facilitate its activation. We showed that this approach actually works; increasing levels of KNC mutant progressively reduce JNK3 activation by co-expressed WT arrestin-3, effectively blocking it at \sim 2:1 molar ratio (Fig. 6A). Although the idea has been proposed that selective elimination of individual arrestin functions by targeted mutagenesis has the potential to create new types of molecular tools for the manipulation of cell signaling (57), our proof-of-principle experiments provide the first demonstration of the effectiveness of this approach. Our data also suggest that mutant forms of arrestins that bind relevant kinases but do not promote the activation of ERK1/2 or p38 can be used to suppress the activation of these signaling cascades.

KNC mutant appears to decrease the activation of both JNK3 (Figs. 2, 3, 4, and 6) and ERK1/2 (Fig. 4), acting as a general suppressor of MAP kinase activity. Interestingly, our data show that another form of arrestin-3, Δ 7 mutant, robustly promotes JNK3 activation (Figs. 2, 3, 4, and 6) while suppressing the phosphorylation of ERK1/2 (Fig. 4). The analysis of the localization of active phospho-JNK in the cell (Fig. 5) shows the limitations associated with subcellular localization of arrestin-3; although the levels of phospho-JNK in the cytoplasm were significantly reduced in the presence of KNC, nuclear phospho-JNK did not seem to be affected (Fig. 5). These data also suggest a way of overcoming this limitation; inactivation of the nuclear export signal in arrestin-3 by a point mutation results in its even dis-

tribution between the nucleus and the cytoplasm (15, 17, 47), suggesting that KNC with a disabled nuclear export signal might be effective in both compartments. This idea needs to be tested experimentally. Although the first generation of arrestin-based tools for manipulation of MAP kinase activity is not perfect, our data prove that this effect can be achieved in living cells. Considering that MAP kinases play key roles in cell proliferation, differentiation, and apoptosis (31, 55), our results demonstrate the feasibility of the construction of novel molecular tools affecting cell behavior and fate. The strategy of creating silent scaffolds described here can be extended to other proteins organizing MAP kinase modules as well as other multiprotein complexes playing key roles in cell signaling.

Acknowledgments—We are grateful to Dr. Jonathan A. Javitch (Columbia University) for expert advice on BRET and the plasmid encoding Venus, Dr. Nevin A. Lambert (Georgia Health Sciences University) for plasmid encoding Renilla luciferase variant 8, and Dr. Borden Lacy (Vanderbilt University) for the use of Synergy 4 microplate reader.

REFERENCES

- Gurevich, V. V., and Gurevich, E. V. (2006) The structural basis of arrestin-mediated regulation of G-protein-coupled receptors. *Pharmacol. Ther.* **110**, 465–502
- Carman, C. V., and Benovic, J. L. (1998) G-protein-coupled receptors. Turn-ons and turn-offs. *Curr. Opin. Neurobiol.* **8**, 335–344
- Gurevich, E. V., and Gurevich, V. V. (2006) Arrestins. Ubiquitous regulators of cellular signaling pathways. *Genome Biology* **7**, 236
- DeWire, S. M., Ahn, S., Lefkowitz, R. J., and Shenoy, S. K. (2007) β -Arrestins and cell signaling. *Annu. Rev. Physiol.* **69**, 483–510
- Burack, W. R., and Shaw, A. S. (2000) Signal transduction. Hanging on a scaffold. *Curr. Opin. Cell Biol.* **12**, 211–216
- Pearson, G., Robinson, F., Beers Gibson, T., Xu, B. E., Karandikar, M., Berman, K., and Cobb, M. H. (2001) Mitogen-activated protein (MAP) kinase pathways. Regulation and physiological functions. *Endocr. Rev.* **22**, 153–183
- McDonald, P. H., Chow, C. W., Miller, W. E., Laporte, S. A., Field, M. E., Lin, F. T., Davis, R. J., and Lefkowitz, R. J. (2000) Beta-arrestin 2: a receptor-regulated MAPK scaffold for the activation of JNK3. *Science* **290**, 1574–1577
- Luttrell, L. M., Roudabush, F. L., Choy, E. W., Miller, W. E., Field, M. E., Pierce, K. L., and Lefkowitz, R. J. (2001) Activation and targeting of extracellular signal-regulated kinases by β -arrestin scaffolds. *Proc. Natl. Acad. Sci. U.S.A.* **98**, 2449–2454
- Bruchas, M. R., Macey, T. A., Lowe, J. D., and Chavkin, C. (2006) κ -Opioid receptor activation of p38 MAPK is GRK3- and arrestin-dependent in neurons and astrocytes. *J. Biol. Chem.* **281**, 18081–18089
- Davis, R. J. (2000) Signal transduction by the JNK group of MAP kinases. *Cell* **103**, 239–252
- Miller, W. E., McDonald, P. H., Cai, S. F., Field, M. E., Davis, R. J., and Lefkowitz, R. J. (2001) Identification of a motif in the carboxyl terminus of β -arrestin2 responsible for activation of JNK3. *J. Biol. Chem.* **276**, 27770–27777
- Song, X., Coffa, S., Fu, H., and Gurevich, V. V. (2009) How does arrestin assemble MAPKs into a signaling complex? *J. Biol. Chem.* **284**, 685–695
- Seo, J., Tsakem, E. L., Breitman, M., and Gurevich, V. V. (2011) Identification of arrestin-3-specific residues necessary for JNK3 kinase activation. *J. Biol. Chem.* **286**, 27894–27901
- Zhan, X., Kaoud, T. S., Dalby, K. N., and Gurevich, V. V. (2011) Nonvisual arrestins function as simple scaffolds assembling the MKK4-JNK3 α 2 signaling complex. *Biochemistry* **50**, 10520–10529
- Song, X., Raman, D., Gurevich, E. V., Vishnivetskiy, S. A., and Gurevich, V. V. (2006) Visual and both non-visual arrestins in their “inactive” conformation bind JNK3 and Mdm2 and relocalize them from the nucleus to the cytoplasm. *J. Biol. Chem.* **281**, 21491–21499
- Song, X., Gurevich, E. V., and Gurevich, V. V. (2007) Cone arrestin binding to JNK3 and Mdm2. Conformational preference and localization of interaction sites. *J. Neurochem.* **103**, 1053–1062
- Scott, M. G., Le Rouzic, E., Périanian, A., Pierotti, V., Ensen, H., Benichou, S., Marullo, S., and Benmerah, A. (2002) Differential nucleocytoplasmic shuttling of β -arrestins. Characterization of a leucine-rich nuclear export signal in β -arrestin2. *J. Biol. Chem.* **277**, 37693–37701
- Vishnivetskiy, S. A., Gimenez, L. E., Francis, D. J., Hanson, S. M., Hubbell, W. L., Klug, C. S., and Gurevich, V. V. (2011) Few residues within an extensive binding interface drive receptor interaction and determine the specificity of arrestin proteins. *J. Biol. Chem.* **286**, 24288–24299
- Zhan, X., Gimenez, L. E., Gurevich, V. V., and Spiller, B. W. (2011) Crystal structure of arrestin-3 reveals the basis of the difference in receptor binding between two non-visual subtypes. *J. Mol. Biol.* **406**, 467–478
- Sterne-Marr, R., Gurevich, V. V., Goldsmith, P., Bodine, R. C., Sanders, C., Donoso, L. A., and Benovic, J. L. (1993) Polypeptide variants of β -arrestin and arrestin3. *J. Biol. Chem.* **268**, 15640–15648
- Pan, L., Gurevich, E. V., and Gurevich, V. V. (2003) The nature of the arrestin x receptor complex determines the ultimate fate of the internalized receptor. *J. Biol. Chem.* **278**, 11623–11632
- Carter, J. M., Gurevich, V. V., Prossnitz, E. R., and Engen, J. R. (2005) Conformational differences between arrestin2 and pre-activated mutants as revealed by hydrogen exchange mass spectrometry. *J. Mol. Biol.* **351**, 865–878
- Celver, J., Vishnivetskiy, S. A., Chavkin, C., and Gurevich, V. V. (2002) Conservation of the phosphate-sensitive elements in the arrestin family of proteins. *J. Biol. Chem.* **277**, 9043–9048
- Hanson, S. M., Cleghorn, W. M., Francis, D. J., Vishnivetskiy, S. A., Raman, D., Song, X., Nair, K. S., Slepak, V. Z., Klug, C. S., and Gurevich, V. V. (2007) Arrestin mobilizes signaling proteins to the cytoskeleton and redirects their activity. *J. Mol. Biol.* **368**, 375–387
- Gimenez, L. E., Kook, S., Vishnivetskiy, S. A., Ahmed, M. R., Gurevich, E. V., and Gurevich, V. V. (2012) Role of receptor-attached phosphates in binding of visual and non-visual arrestins to G protein-coupled receptors. *J. Biol. Chem.* **287**, 9028–9040
- Loening, A. M., Fenn, T. D., Wu, A. M., and Gambhir, S. S. (2006) Consensus guided mutagenesis of Renilla luciferase yields enhanced stability and light output. *Protein Eng. Des. Sel.* **19**, 391–400
- Azzi, M., Charest, P. G., Angers, S., Rousseau, G., Kohout, T., Bouvier, M., and Piñeyro, G. (2003) β -Arrestin-mediated activation of MAPK by inverse agonists reveals distinct active conformations for G protein-coupled receptors. *Proc. Natl. Acad. Sci. U.S.A.* **100**, 11406–11411
- Coffa, S., Breitman, M., Hanson, S. M., Callaway, K., Kook, S., Dalby, K. N., and Gurevich, V. V. (2011) The effect of arrestin conformation on the recruitment of c-Raf1, MEK1, and ERK1/2 activation. *PLoS One* **6**, e28723
- Wacker, W. B., Donoso, L. A., Kalsow, C. M., Yankeelov, J. A., Jr., and Organisciak, D. T. (1977) Experimental allergic uveitis. Isolation, characterization, and localization of a soluble uveitopathogenic antigen from bovine retina. *J. Immunol.* **119**, 1949–1958
- Song, X., Vishnivetskiy, S. A., Gross, O. P., Emelianoff, K., Mendez, A., Chen, J., Gurevich, E. V., Burns, M. E., and Gurevich, V. V. (2009) Enhanced arrestin facilitates recovery and protects rods lacking rhodopsin phosphorylation. *Curr. Biol.* **19**, 700–705
- Keshet, Y., and Seger, R. (2010) The MAP kinase signaling cascades. A system of hundreds of components regulates a diverse array of physiological functions. *Methods Mol. Biol.* **661**, 3–38
- Vishnivetskiy, S. A., Francis, D., Van Eps, N., Kim, M., Hanson, S. M., Klug, C. S., Hubbell, W. L., and Gurevich, V. V. (2010) The role of arrestin α -helix I in receptor binding. *J. Mol. Biol.* **395**, 42–54
- Hanson, S. M., Francis, D. J., Vishnivetskiy, S. A., Kolobova, E. A., Hubbell, W. L., Klug, C. S., and Gurevich, V. V. (2006) Differential interaction of spin-labeled arrestin with inactive and active phosphorhodopsin. *Proc. Natl. Acad. Sci. U.S.A.* **103**, 4900–4905
- Vishnivetskiy, S. A., Hirsch, J. A., Velez, M. G., Gurevich, Y. V., and Gurevich, V. V. (2002) Transition of arrestin into the active receptor binding state requires an extended interdomain hinge. *J. Biol. Chem.* **277**,

- 43961–43967
35. Vishnivetskiy, S. A., Schubert, C., Climaco, G. C., Gurevich, V. V., Velez, M. G., and Gurevich, V. V. (2000) An additional phosphate binding element in arrestin molecule. Implications for the mechanism of arrestin activation. *J. Biol. Chem.* **275**, 41049–41057
 36. Hamdan, F. F., Rochdi, M. D., Breton, B., Fessart, D., Michaud, D. E., Charest, P. G., Laporte, S. A., and Bouvier, M. (2007) Unraveling G protein-coupled receptor endocytosis pathways using real-time monitoring of agonist-promoted interaction between β -arrestins and AP-2. *J. Biol. Chem.* **282**, 29089–29100
 37. Gurevich, V. V., and Gurevich, E. V. (2004) The molecular acrobatics of arrestin activation. *Trends Pharmacol. Sci.* **25**, 105–111
 38. Goodman, O. B., Jr., Krupnick, J. G., Santini, F., Gurevich, V. V., Penn, R. B., Gagnon, A. W., Keen, J. H., and Benovic, J. L. (1996) β -Arrestin acts as a clathrin adaptor in endocytosis of the β 2-adrenergic receptor. *Nature* **383**, 447–450
 39. Laporte, S. A., Oakley, R. H., Zhang, J., Holt, J. A., Ferguson, S. S., Caron, M. G., and Barak, L. S. (1999) The β 2-adrenergic receptor/ β -arrestin complex recruits the clathrin adaptor AP-2 during endocytosis. *Proc. Natl. Acad. Sci. U.S.A.* **96**, 3712–3717
 40. Walther, C., Nagel, S., Gimenez, L. E., Mörl, K., Gurevich, V. V., and Beck-Sickinger, A. G. (2010) Ligand-induced internalization and recycling of the human neuropeptide Y2 receptor is regulated by its carboxyl-terminal tail. *J. Biol. Chem.* **285**, 41578–41590
 41. Namkung, Y., Dipace, C., Javitch, J. A., and Sibley, D. R. (2009) G protein-coupled receptor kinase-mediated phosphorylation regulates post-endocytic trafficking of the D2 dopamine receptor. *J. Biol. Chem.* **284**, 15038–15051
 42. James, J. R., Oliveira, M. I., Carmo, A. M., Iaboni, A., and Davis, S. J. (2006) A rigorous experimental framework for detecting protein oligomerization using bioluminescence resonance energy transfer. *Nat. Methods* **3**, 1001–1006
 43. Guo, W., Urizar, E., Kralikova, M., Mobarec, J. C., Shi, L., Filizola, M., and Javitch, J. A. (2008) Dopamine D2 receptors form higher order oligomers at physiological expression levels. *EMBO J.* **27**, 2293–2304
 44. Guo, C., and Whitmarsh, A. J. (2008) The β -arrestin-2 scaffold protein promotes c-Jun N-terminal kinase-3 activation by binding to its nonconserved N terminus. *J. Biol. Chem.* **283**, 15903–15911
 45. Stork, P. J., and Schmitt, J. M. (2002) Cross-talk between cAMP and MAP kinase signaling in the regulation of cell proliferation. *Trends Cell Biol.* **12**, 258–266
 46. Coffa, S., Breitman, M., Spiller, B. W., and Gurevich, V. V. (2011) A single mutation in arrestin-2 prevents ERK1/2 activation by reducing c-Raf1 binding. *Biochemistry* **50**, 6951–6958
 47. Wang, P., Wu, Y., Ge, X., Ma, L., and Pei, G. (2003) Subcellular localization of β -arrestins is determined by their intact N domain and the nuclear export signal at the C terminus. *J. Biol. Chem.* **278**, 11648–11653
 48. Turjanski, A. G., Vaqué, J. P., and Gutkind, J. S. (2007) MAP kinases and the control of nuclear events. *Oncogene* **26**, 3240–3253
 49. Gupta, S., Barrett, T., Whitmarsh, A. J., Cavanagh, J., Sluss, H. K., Dérijard, B., and Davis, R. J. (1996) Selective interaction of JNK protein kinase isoforms with transcription factors. *EMBO J.* **15**, 2760–2770
 50. Dacres, H., Wang, J., Dumancic, M. M., and Trowell, S. C. (2010) Experimental determination of the Förster distance for two commonly used bioluminescent resonance energy transfer pairs. *Anal. Chem.* **82**, 432–435
 51. Lohse, M. J., Bünemann, M., Hoffmann, C., Vilardaga, J. P., and Nikolaev, V. O. (2007) Monitoring receptor signaling by intramolecular FRET. *Curr. Opin. Pharmacol.* **7**, 547–553
 52. Hirsch, J. A., Schubert, C., Gurevich, V. V., and Sigler, P. B. (1999) The 2.8 Å crystal structure of visual arrestin. A model for arrestin regulation. *Cell* **97**, 257–269
 53. Han, M., Gurevich, V. V., Vishnivetskiy, S. A., Sigler, P. B., and Schubert, C. (2001) Crystal structure of β -arrestin at 1.9 Å. Possible mechanism of receptor binding and membrane translocation. *Structure* **9**, 869–880
 54. Sutton, R. B., Vishnivetskiy, S. A., Robert, J., Hanson, S. M., Raman, D., Knox, B. E., Kono, M., Navarro, J., and Gurevich, V. V. (2005) Crystal structure of cone arrestin at 2.3 Å. Evolution of receptor specificity. *J. Mol. Biol.* **354**, 1069–1080
 55. Winter-Vann, A. M., and Johnson, G. L. (2007) Integrated activation of MAP3Ks balances cell fate in response to stress. *J. Cell Biochem.* **102**, 848–858
 56. Dhanasekaran, D. N., Kashef, K., Lee, C. M., Xu, H., and Reddy, E. P. (2007) Scaffold proteins of MAP-kinase modules. *Oncogene* **26**, 3185–3202
 57. Gurevich, V. V., and Gurevich, E. V. (2010) Custom-designed proteins as novel therapeutic tools? The case of arrestins. *Expert Rev. Mol. Med.* **12**, e13